Article

Extending the Hierarchy of Heterogeneous Catalysis to Substituted Derivatives of Benzimidazole Synthesis: Transition Metals Decorated CNTs

Zahoor Iqbal [1], Saima Sadiq [1,2], Muhammad Sadiq [1,*] , Inam Ullah [1], Zahid Fazal [1], Doctor Khan [1], Neelam Bibi [1], Khalid Saeed [3], Adnan Ali Khan [4], Fazal Mabood [5] and Mumtaz Ali [1]

[1] Department of Chemistry, University of Malakand, Chakdara 18800, Pakistan; arhamiqbal2017@gmail.com (Z.I.); saima@knu.ac.kr (S.S.); inamullah847@gmail.com (I.U.); zahidhashami123@gmail.com (Z.F.); khandoctor3454@gmail.com (D.K.); nelambibi190@gmail.com (N.B.); mumtazali@uom.edu.pk (M.A.)
[2] School of Applied Chemical Engineering, Kyungpook National University, Daegu 41566, Korea
[3] Department of Chemistry, Bacha Khan University, Charsadda 24420, Pakistan; khalidkhalil2002@yahoo.com
[4] Center for Computational Materials Science, University of Malakand, Chakdara 18800, Pakistan; aak95287@gmail.com
[5] Department of Biological Sciences and Chemistry College of Arts and Sciences, University of Nizwa, Nizwa 616, Oman; mehboob@unizwa.edu.om
[*] Correspondence: sadiq@uom.edu.pk or mohammad_sadiq26@yahoo.com; Tel.: +92-945-763441

Abstract: A simple and practical procedure has been adopted for one pot synthesis of benzimidazole derivatives under mild reaction conditions, starting from cinnamyl alcohol (COH) with bimetallic nanoparticles (BNPs) and supported bimetallic nanoparticles of Cu, Ti, Zn, Mn, Ag, and Co. All the catalysts were characterized by Scanning Electron Microscopy (SEM), Energy Dispersive X-ray Spectroscopy (EDX), X-Ray Diffractometry (XRD), Brunauer Emmett-Teller (BET) surface area, and pore size analyzer. The products were identified/quantified with ^{1}HNMR, FT-IR, and MS. 98% yield of substituted derivatives of benzimidazole was obtained with Cu–Ti supported on FMWCNTs in ethanol with excellent selectivity. Quantum chemical calculations of molecular reactivity of substituted cinnamaldehyde (CHO) and ortho phenylenediamine (OPD) have good consistency with experimental results. The returns of this work were the use of readily available catalysts, high yield, short reaction time, and simplicity of the process.

Keywords: cinnamyl alcohol; cinnamaldehyde; benzimidazole; nanoparticles/FMWCNTs

1. Introduction

In heterocyclic aromatic organic compounds, benzimidazole is an important moiety which is made up of the fusion of benzene and imidazole rings [1]. In order to develop molecules of medicinal and biological importance among heterocycles containing a nitrogen atom, benzimidazole and its substituted derivatives are considered important intermediates [2]. Benzimidazoles have commercial importance especially, in veterinarian medicines, for example, treatment of ulcers, as antihelminth agents and as antihistamines [3–6].

Substituted derivatives of benzimidazoles have gained much attraction for the community of synthetic organic chemists, therefore they are using catalytic technology for the synthesis of these heterocyclic compounds. For the synthesis of benzimidazoles, different synthetic methods have been reported such as reaction of ortho phenylenediamine (OPD) with carboxylic acids, aldehydes and their

substituted derivatives. Variety of catalysts such as lanthanum chloride [7], solid Co(OH)$_2$ and CoO (II) [8], ammonium chloride [9], alumina, silica gel and zeolite HY [10], indium triflate [In(OTf)$_3$] [11], zinc triflate [12], polyphosphoric acid (PPA) [13], animal bone meal (ABM) and Lewis acids doped ABMs [14], oxalic acid [15], aminoxyl radical [16], heteropoly acids (HPAs) [17], L-proline [18], and polyaniline-sulfate salt [19] have been used for the synthesis of benzimidazole derivatives under a multiplicity of reaction conditions.

Reddy et al. [20] have reported the fluctuation of chemical reactivity of aryl halides with substitution toward the synthesis of benzimidazole. The percentage yield was boost up with electron withdrawing groups attach to aryl halides. Similarly, structural and electronic properties of substituted aniline was predicted by DFT-B3LYP/6-311++ G (d, p) level of theory and reveals that methoxy-aniline has more nucleophilic character, less value of hardness, and has greater reactivity than other derivatives of aniline towards nucleophilic addition with benzaldehyde [21]. This provokes us to study chemical reactivity of substituted derivatives of substituted cinnamaldehyde (CHO) and OPD with Density Functional Theory (DFT).

Recently, for the synthesis of substituted derivatives of benzimidazole, heterogeneous and homogeneous catalysis have gained extensive attraction due to the advantageous approach of these techniques which include easy availability, simple handling, and easy workup [22]. However, most of these methods have some limitations, for example laborious workup procedure, long reaction times, high temperature, use of expensive catalyst, by-product formation, low yields, and elevated reaction conditions [23–27]. Therefore, it is necessary to introduce new methods or extend the prevailing ones to overcome these mentioned difficulties or limitations via new catalytic methods for the synthesis of substituted derivatives. In the present study, we are going to use easily available, less toxic, reusable, and low-cost catalysts combined with a simple procedure, to provide an economic and waste-free chemical method for the synthesis of benzimidazole derivatives and simple descriptor will be developed for investigating the effect of substitution on the molecular reactivity of CHO and OPD using density functional theory with B3LYP/6-311++ G (d, p).

2. Results and Discussion

2.1. Physical Characterization of the Catalysts

The SEM images of the pure Zn–Mn NPs and Zn–Mn/FMWCNTs (Figure S1a,b) reveals that Zn–Mn NPs are present in the form of agglomerates while well dispersed when supported on FMWCNTs. The EDX spectra of Zn Mn NPs (Figure S1c,d) show that the major elements are Zn and Mn while in case of Zn–Mn/FMWCNTs also possess peaks for carbon and oxygen. XRD patterns of Zn–Mn NPs and Zn–Mn/ FMWCNTs (Figure S1e,f) shows that the long peaks placed at 36° while small peaks were appeared at 34° and 48.5° indexed to the hexagonal wurtzite phase of ZnO. The formation of crystalline MnO$_2$ nanoparticles was confirmed by the peak appeared at 23° and 33° and 66° while the peaks appeared at 44.5° and 60° indexed the formation of tetragonal Mn$_3$O$_4$. The particle size of Zn–Mn NPs calculated from SEM and XRD were 33.8 nm and 30.5 nm (Table 1, entry 1) while the surface area of Zn–Mn NPs and Zn–Mn/FMWCNTs were 34.5 m^2/g and 229.3 m^2/g (Table 1, entries 1 and 2), respectively [28].

Table 1. Particle size, morphology, X Ray Diffractions, and BET surface area of the prepared catalysts.

S.No	Catalyst	SEM	nm *	Morphology	XRD	2θ Values	nm **	BET (m²/g)
1	Zn–Mn	S1(a)	33.8	Agglomerated	S1(e)	34.5°,37.1°,48°,61°,65.6°,75.1°	30.5	34.5
2	Zn–Mn/FMWCNTs	S1(b)	-	Dispersed and Agglomerated	S1 (f)	34.5°,37.1°,48°,53.5°,61.3°,75.15°,79°	-	229.3
3	Ag–Co	S2(a)	27.5	Dispersed	S2 (e)	32.8°,33.6°,38.1°,44.2°,55.2°,77.3°	28.2	27.3
4	Ag–Co/FMWCNTs	S2(b)	-	Dispersed and Agglomerated	S2(f)	18.5°,32.8°,33.6°,33.7°,38.1°,38.2°,44°, 56.3°,77.3°	-	231.5
5	Cu–Ti	S3(a)	22.7	Irregular shaped	S3 (e)	25.3°,35°,38.6°,48.1°,54°	23.5	31.8
6	Cu–Ti/FMWCNTs	S3(b)	-	Dispersed and agglomerated	S3 (f)	25.3°,35°,38°,48.1°,54°,63°	-	230.1
7	Co–Ti	S4(a)	22.3	Dispersed	S4 (e)	25.15°,38.45°,48°,54°,4°,69°,70°,76°	22.9	26.4
8	Co–Ti/FMWCNTs	S4(b)	-	Dispersed	S4 (f)	25.3°,37.7°,48°,54°,64°,76°	-	233.7

* Average particle size calculated from SEM images by average grain intercept (AGI) method, ** Particle size calculated from XRD by the Scherrer Equation ($\tau = \frac{K\lambda}{\beta cos\theta}$).
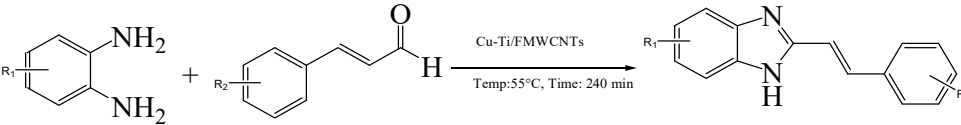
The SEM images of Ag–Co NPs and Ag–Co/FMWCNTs were shown by (Figure S2a,b). The Ag–Co NPs are smooth and segregated. Similarly, SEM micrograph of Ag–Co/FMWCNTs show that the NPs are well dispersed on the surface of FMWCNTs. The EDX spectra of Ag–Co NPs and Ag–Co/FMWCNTs (Figure S2c,d) reflects presence of Ag and Co in the case of NPs while carbon and oxygen in the case of supported BNPs. XRD patterns (Figure S2e,f) of Ag–Co NPs and Ag–Co/FMWCNTs shows that the long peaks placed at 32.85°, 33.65°, 38.1°, 44.25°, 55.25°, and 77.35° which are the characteristic peaks of Ag and Co NPs. The particle size of Ag–Co NPs calculated from SEM and XRD (Table 1, entry 3) were 27.5 nm and 28.2 nm while the surface area of Ag–Co NPs and Ag–Co/FMWCNTs were 27.3 m^2/g and 231.5 m^2/g (Table 1, entries 3 and 4), respectively [29].

The SEM images of Cu–Ti NPs and Cu–Ti/FMWCNTs were presented by (Figure S3a,b) which reveal that Cu–Ti NPs are mostly irregular and dispersed. Similarly, SEM micrograph of Cu–Ti /FMWCNTs showed that Cu–Ti NPs are dispersed/aggregated on the surface of FMWCNTs. The EDX spectra (Figure S3c,d) show that in both catalysts, Cu and Ti are present in large quantity, while the carbon and oxygen peaks appeared in Cu–Ti/FMWCNTs due to FMWCNTs. The presence of oxygen peaks indicates the formation of metal oxides and functionalization of MWCNTs during acid treatment, which introduced carboxylic functional group. From the XRD patterns of the Cu–Ti NPs and Cu–Ti/FMWCNT (Figure S3e,f), characteristic peaks appeared at 25.3° and 48.1° shows the anatase phase of TiO_2 NPs, clarifying the absence of brookite and the rutile phase of titania. The XRD spectrum also gives peaks at about 35° and 54°, which shows that the copper oxide NPs are also formed successfully. The particle size of Cu–Ti NPs calculated from SEM and XRD were 22.7 nm and 23.5 nm (Table 1, entry 5) while the surface area of Cu–Ti NPs and Cu–Ti/FMWCNTs were 31.8 m^2/g and 230.1 m^2/g (Table 1, entries 5 and 6), respectively [30].

The SEM images of Co–Ti NPs and Co–Ti/FMWCNTs were given by (Figure S4a,b) which reflect smooth morphology of BNPs. The SEM micrograph of Co–Ti/FMWCNTs shows that the Co–Ti NPs are well dispersed on the surface of FMWCNTs. The EDX spectra (Figure S4c,d) reveal that in both catalysts, Co and Ti are present in large quantity, while due to FMWCNTs carbon and oxygen peaks appeared in Co–Ti/FMWCNTs. XRD patterns of the Co–Ti NPs and Co–Ti/FMWCNT (Figure S4e,f) show characteristic peaks appeared at 25.15°, 38.45°, 48°, 54°, 64°, 69°, 70°, and 76° responsible for Co–Ti and Co–Ti/FMWCNTs. The particle size of Co–Ti NPs calculated from SEM and XRD were 22.3 nm and 22.9 nm (Table 1, entry 7) while the surface area of Co–Ti NPs and Co–Ti/FMWCNTs were 26.4 m^2/g and 233.7 m^2/g (Table 1, entries 7 and 8), respectively [31]

2.2. Catalysts Screening

The conversion of COH to CHO (yield; 99.2%, selectivity 99.9%) was carried out in different solvents (ethanol, n-hexane, acetonitrile, and water) under the optimized set of reaction parameters such as Cat; 0.1 g, COH; 120 mg (0.89 mmol) in 10 mL solvent, Time; 60 min, Temp; 70 °C, Stirring; 1200 rpm; Oxidant; O_2 (1 atm). After the completion of COH to CHO oxidation, reactor was flushed with N_2 and OPD were loaded to the same reactor. Although the reaction between substituted OPD and CHO were also investigated under vigorous stirring to obtain substituted derivatives of benzimidazole as shown in Table 2. The same reaction was also investigated in different solvents such as ethanol, n-hexane, and acetonitrile. The blank test for the reaction of CHO and OPD was performed under same set of reaction parameters in the absence of catalyst. A small amount of product was observed even after a long time. Similarly, the reaction was repeated with FMWCNTs in ethanol under the same set reaction parameters without convincing yield after 4 h. The IR (KBr) υ values were as follows: 3377, 3027, 2924, 2853, 1948, 1805, 1633, 1598, 1495, 1449, 1402, 1355,1326, 1284, 1194, 1153, 1070, 1018, 963, 918, 841, 737, 691, and 558 cm^{-1} as shown by Figure S5 and melting point was 198–202 °C with 73% yield. The Electron Impact Mass Spectrometry (EIMS) m/z values were (% relative abundance): 221 (M+), 194, 173,155,144, and 134 as shown by Figure S6. ^{1}HNMR (600 MHz, DMSO): δ 7.0–8.3 m (9H, Ar–H), 6.6–6.9 d (2H, CH=CH), 5.3 m (1H, NH) as shown in Figure S7. The results are in close agreement with reported literature [32].

Table 2. Synthesis of benzimidazoles from substituted OPD and CHO in ethanol.

ENTRY	R_1	R_2	% Yield
1	H	H	73
2	4-OMe	4-NO_2	98
3	4-OMe	4-Cl	95
4	4-OMe	3-Me	82
5	4-OMe	3-OMe	77
6	4-Me	4-NO_2	94
7	4-Me	4-Cl	92
8	4-Me	3-Me	76
9	4-Me	3-OMe	69
10	4-Cl	3-OMe	66
11	4-Cl	3-Me	71
12	4-Cl	4-NO_2	88
13	4-NO_2	3-Cl	84
14	4-NO_2	3-Me	65
15	4-NO_2	3-OMe	61

2.3. Time Profile Study

For the cyclization of OPD and CHO, BNPs and BNPs/FMWCNTs were used in the time range 60–240 min while keeping other parameters constant. The time effect on the percent yield in catalytic synthesis of benzimidazole and its substituted derivatives shows linear correlation with reaction duration due to the interaction of OPD and CHO with the active sites of the catalyst as given in the Figure 1. It is clear from Table S1 that Cu–Ti/FMWCNTs was the most efficient catalyst which give maximum yield of 98% after 240 min. Comparative studies of reported and current catalysts are presented in Table 3. Nagaraju and coworkers [32] claimed 92% yield with reasonable selectivity to desire products with Mn/ZrO$_2$ in ethanol but the high temperature of the reaction makes it open for further investigation. Similarly, graphene oxide was efficiently used for benzimidazole synthesis in methanol from CHO and OPD at 60 °C in 4 h [33]. However, the process is unfavorable for large scale synthesis due to the use of toxic solvent. In the current project, we have reported the cyclization of OPD and CHO to substituted derivatives of benzimidazole at 55 °C in ethanol after 240 min with a maximum yield of 98%.
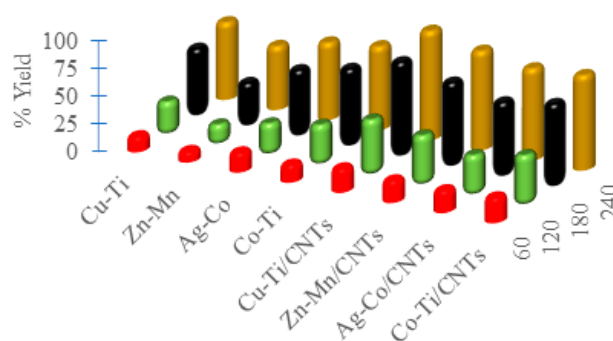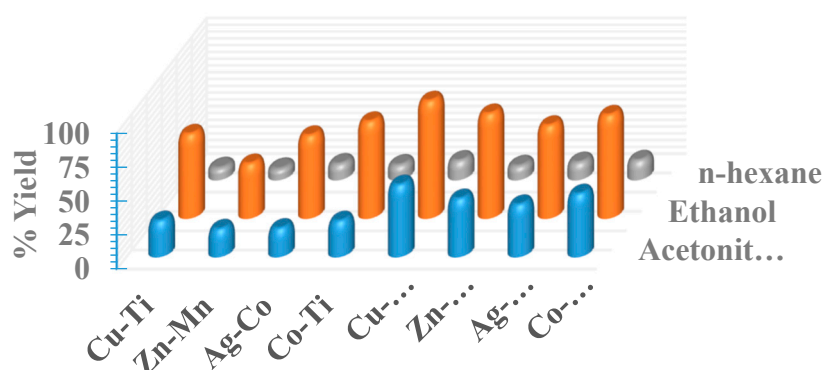

Figure 1. Effect of time on the percentage yield of substituted derivatives of benzimidazole over 0.1 g of catalysts in ethanol at 55 °C.

Table 3. Comparison of the catalytic activity of reported catalysts with the present one, being used for the synthesis of benzimidazoles from cinnamaldehyde and ortho phenylenediamine.

Catalyst	Reaction Conditions	% Yield	Reference
Co/SBA-15 nanocatalyst (0.014 g)	CHO (1 mmol), OPD (1 mmol), EtOH (2 mL), temp (60 °C), time (4 h)	98	[34]
Graphene Oxide (0.02 g)	CHO (1 mmol), OPD (1 mmol), MeOH (3 mL), temp (60 °C), time (4 h)	81	[33]
Silica sulfuric acid (0.05 g)	Orthoester (1.1 mmol), OPD (1 mmol), solvent free, temp (85 °C), time (5 h)	90	[35]
MnZrO$_2$ (0.2 g)	CHO (1mmol), OPD (1 mmol), EtOH (5 mL), temp (80 °C), time (2 h)	92	[32]
Cu–Ti/FMWCNTs (0.1 g)	CHO (0.89 mmol), OPD (1.07 mmol), EtOH (10 mL), temp (55 °C), time (4 h)	98	Present Study

2.4. Solvent Effect

The effect of different solvents: ethanol, acetonitrile, and n-hexane were investigated on the percentage yield of isolated product. The reaction was found more efficient in ethanol as compared to other solvents as shown in Figure 2. Acetonitrile and n-hexane resulted in a lower yield while water can also be used as a solvent with reasonable yield but limited by reflux conditions due to solubility difficulties of organic molecules and laborious isolation of the products. Synthesis of benzimidazole with a Bronsted acidic ionic liquid while using polar and protic solvents such as ethanol, methanol, dimethyl formamide (DMF), dimethyl sulfoxide (DMSO), and water have investigated elsewhere [36]. They reported good to excellent yield in all solvent except water and also claim a decrease in selectivity of desired products. The reaction was performed in solvent free conditions but in due course of time, reaction was not completed and also showed loss of selectivity to desired products (4a). A similar trend was observed by Baltork et al. [35] while using silica sulfuric acid as a catalyst for synthesis of benzimidazole in solvent free conditions at 85 °C. Nagaraju and co-workers [32] have investigated the use of different solvents e.g., DMSO, DMF, water, methanol, ethanol, chloroform, and acetonitrile for the synthesis of benzimidazole with Mn/ZrO$_2$. They observed that the ethanol was excellent solvent for the synthesis of benzimidazole among other solvents. Similarly, Kalhor et al. [37] investigated the synthesis of benzimidazole from OPD and 4-nitro-benzaldehyde while using different catalysts of hexahydrate, nitrate of copper, nickel, cobalt, iron, and manganese in the presence of different solvents like ethanol, methanol, DMSO, and acetonitrile. They observed a 92% yield with ethanol keeping other parameters constant. In the current study, a 98% yield was achieved with ethanol in the presence of Cu–Ti/FMWCNTs in 240 min at 55 °C.

Figure 2. Effect of solvent on the percentage yield of substituted derivatives of benzimidazole over 0.1 g of catalyst in 240 min at 55 °C.

2.5. Thermal Effect

The thermal effect was explored on percentage yield of 2-styryl-1H-benzo[d]imidazole from OPD and CHO in the range 25–55 °C while using BNPs and BNPs/FMWCNTs in ethanol. With an increase in the temperature, the percentage yield of substituted derivatives of benzimidazole was proportionally increased as shown in Figure 3. The activation energy calculated from Arrhenius equation showed that the temperature has a paramount effect on the rate of reaction, Cu–Ti/FMWCNTs has a less value of activation energy among the applied catalysts with maximum productivity value 2.3 mmolg^{-1}h^{-1} at 55 °C as shown in Figure S8. A similar trend was also observed by Nagaraju et al. [32] in the synthesis of benzimidazole over Mn/ZrO$_2$ in ethanol at a temperature range of 25–100 °C. They achieved maximum yield with high selectivity at 80 °C while at high temperature no increase was observed in conversion, although selectivity to desire product decreases. The correlation of activation energy and productivity clarify the order of catalytic activity of the catalysts being used for the synthesis of substituted derivatives of benzimidazole (Cu–Ti/FMWCNTs > Zn–Mn/FMWCNTs > Co–Ti/FMWCNTs > Ag–Co/FMWCNTs) as presented in Figure 4.
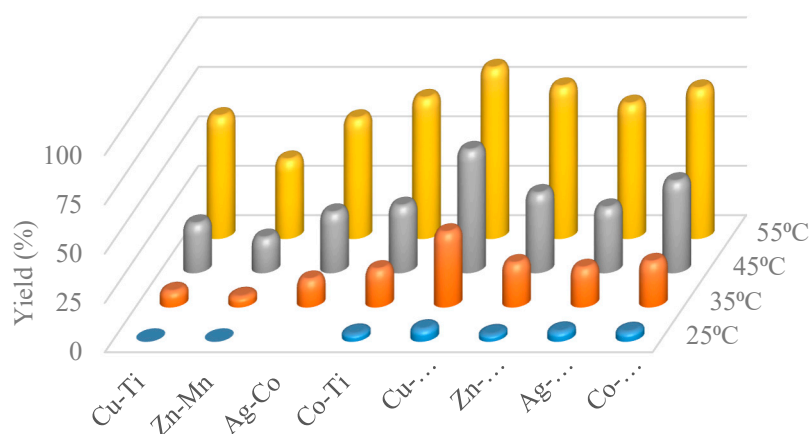

Figure 3. Effect of temperature on the percentage yield of substituted derivatives of benzimidazole in ethanol over 0.1 g of catalyst in 240 min.
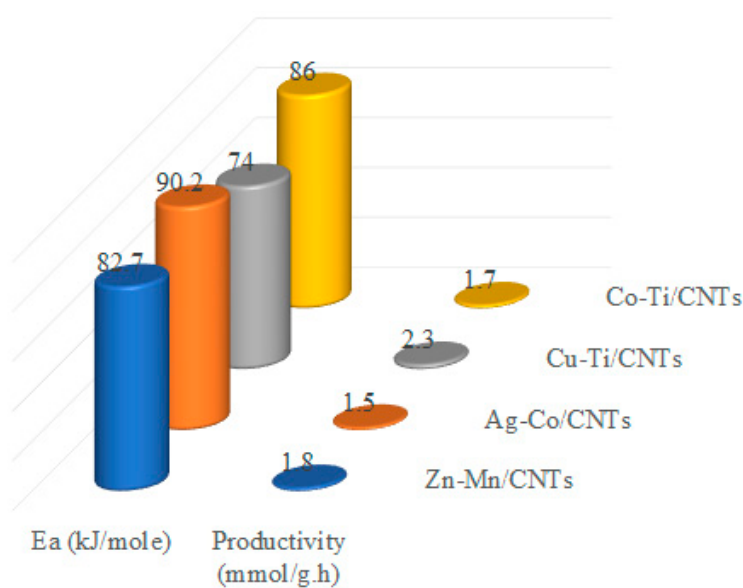

Figure 4. Correlation of activation energy with productivity of benzimidazoles.

2.6. Structural and Electronic Properties

It is clear from the Table S2 that among substituted CHO (electron withdrawing and electron donating groups), 4-NO_2-CHO was more reactive derivative than the other substituted CHO due to the lower values of HOMO-LUMO energy gap as shown in Figure S9 and chemical hardness (η). The greater the electronic chemical potential, the less stable or more reactive the compound will be. Therefore, compound 4-NO_2-CHO is more reactive than all derivatives of CHO due to a greater value of electronic chemical potential as shown in Figure 5a. It has been observed that electron withdrawing groups in the aromatic ring of CHO increase the reaction rate and decrease the reaction time by increasing the electrophilicity. The electrophilicity values (ω) of substituted CHO show that compound 4-NO_2-CHO was the strongest electrophile having a high value of ω. The order of reactivity of the substituted CHO being used for the synthesis of benzimidazoles as presented in Scheme 1.
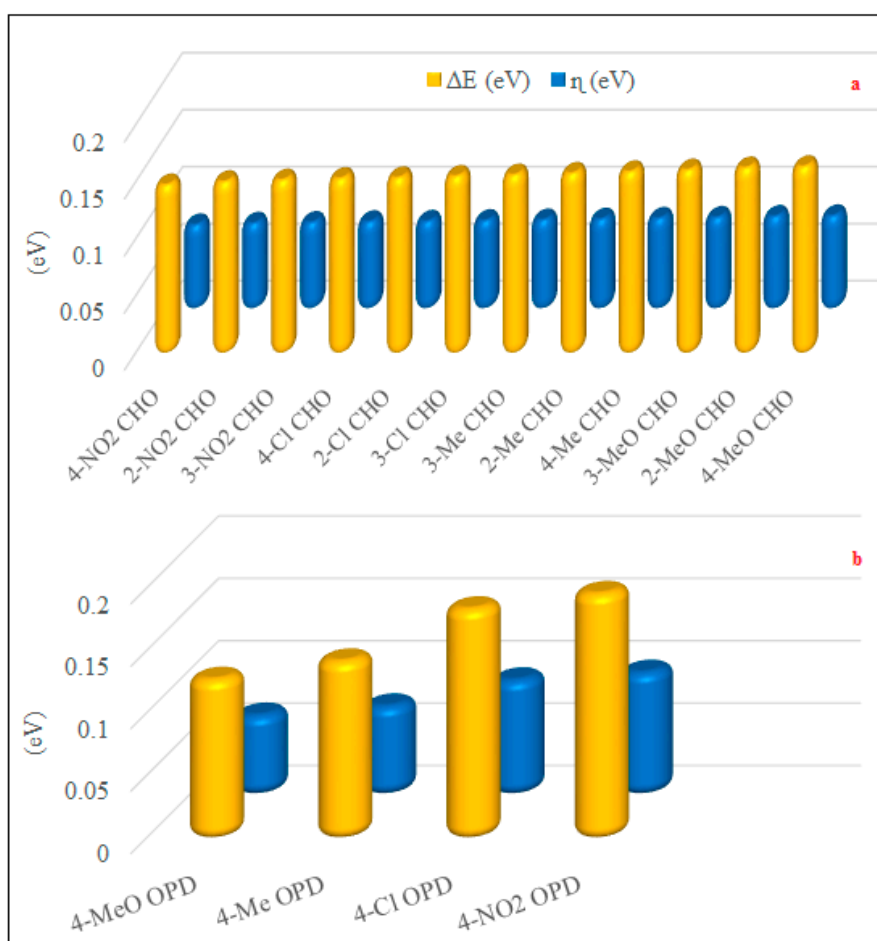

Figure 5. Effect of substitution on the chemical reactivity of (**a**) CHO and (**b**) OPD.

It is clear from Table S3 among different derivatives of OPD (electron withdrawing and electron donating groups), 4-OMe OPD was the more reactive due to low band gap energies as shown in Figure S10 and chemical hardness than all other derivatives of OPD. The greater value of the band gap energies, the molecule will be harder and more stable or less reactive as shown in Figure 5b. It has been observed that electron donating groups in the OPD increase the reaction rate and decrease the reaction time by increasing the nucleophilicity of the OPD. The order of reactivity of the substituted OPD being used for the synthesis of benzimidazoles as presented in Scheme 2.
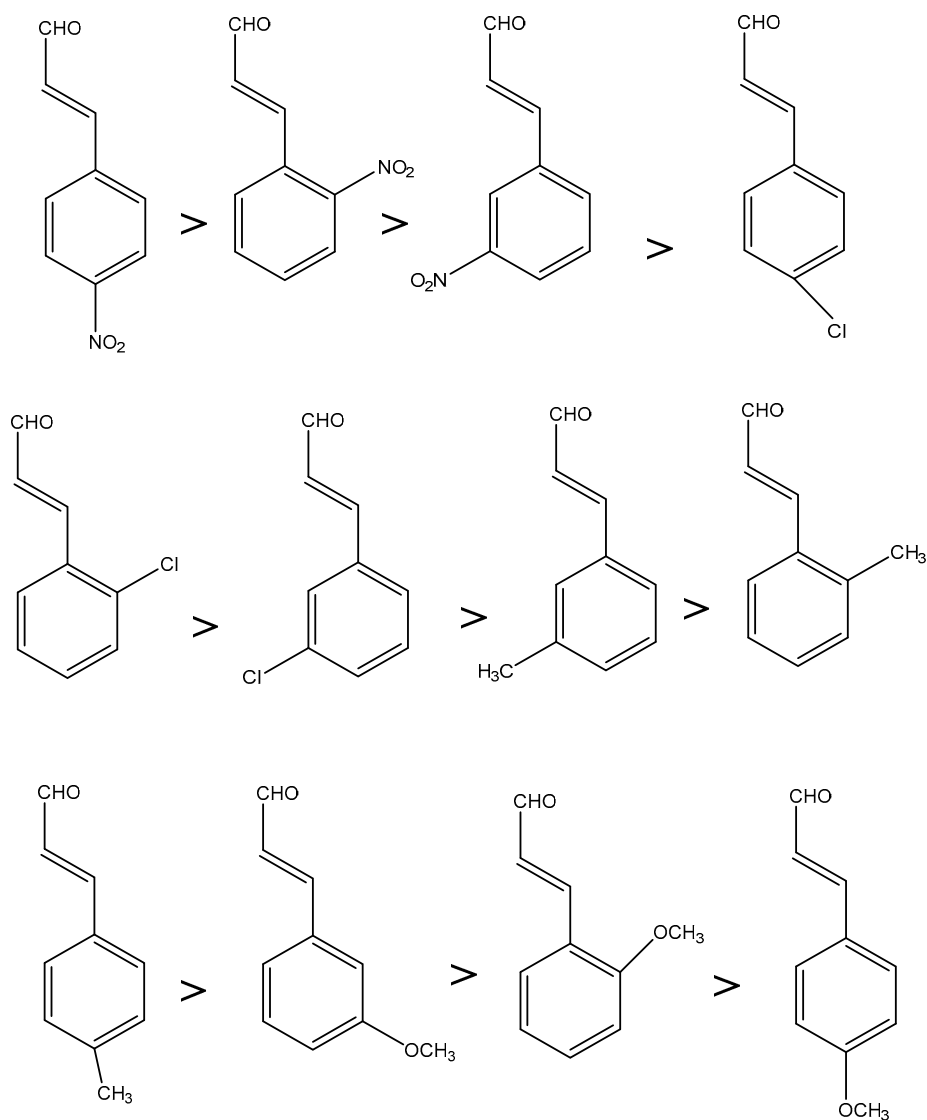
Scheme 1. Order of chemical reactivity of substituted cinnamaldehyde.
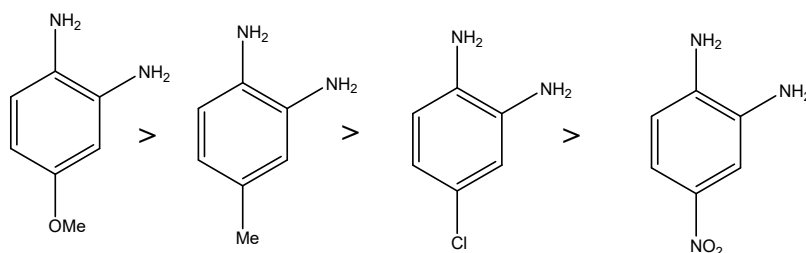
Scheme 2. Order of Chemical Reactivity of Substituted ortho phenylenediamine.

3. Experimental

The chemicals and reagents used in the current study were of high purity and purchased from Merck, Sigma Aldrich, Alfa Aesar and Daejung. Multiwalled carbon nanotubes (MWCNTs; O.D. × L 6–13 nm × 2.5–20 μm) were purchased from Sigma Aldrich. Gases like oxygen and nitrogen were supplied by British Oxygen Company (BOC), Pakistan, Ltd. For the removal of traces from the gases, specific filters (C.R.S.Inc.202268) and (C.R.S.Inc.202223) were used.

3.1. Functionalization of MWCNTs

MWCNTs were refluxed for one hour with para aminobenzoic acid. Functionalized multiwalled carbon nanotubes were separated through centrifugation, washed in modified Soxhlet apparatus (discontinue the circulation of water) with 0.1 N HCl and Millipore water until neutral pH, then dried over night at 110 °C in oven.

3.2. Synthesis of the Nanoparticles

For the synthesis of nanoparticles (NPs) and bimetallic nanoparticles (BNPs), precipitation/co-precipitation methods were adopted respectively. Metal salts (0.01 M) were titrated against base (NH_4OH), dense precipitate of metal hydroxide was filtered, washed with Millipore water and dried.

3.3. Synthesis of Supported Nanoparticles

The prepared nanoparticles (0.1 g) were dispersed in ethanol by sonication (30 min). 0.1g of functionalized multiwalled carbon nanotubes (FMWCNTs) were added to the suspension. The mixture was further sonicated for 30 min. Nanoparticles supported FMWCNTs were separated by centrifugation, washed with Millipore water and dried in oven at 100 °C.

3.4. Characterization of Catalysts

The catalysts were characterized by using Scanning Electron Microscopy (SEM, JSM 5910, JEOL, Tokyo, Japan). Elemental analysis of samples was investigated by Energy Dispersive X-ray Spectroscopy (EDX, JSM 5910, JEOL, Tokyo, Japan). The phase of the catalysts was determined by X-Ray Diffractometer (XRD, JDX-3532, JEOL, Tokyo, Japan) with radiation source CuKα with λ = 0.15418 nm, while operating voltage of 20–40 kV, in the 2θ range of 0–160° at a step size of 0.05°. BET surface area of the BNPs and BNPs/FMWCNTs was measured by using surface area and pore size analyzer (NOVA2200e, Quantachrome, Boynton Beach, FL, USA).

3.5. Catalytic Test

0.1 g of catalyst and 120 mg (0.89 mmol) cinnamyl alcohol in 10 mL solvent, were loaded to three necked double walled round bottom batch reactor equipped with condenser and quick fit thermometer. The reaction mixture was stirred under continuous flow of oxygen at 1 atm (760 torr) while desired temperature was attained by circulation of glycol through the walls of reactor. Product of alcohol oxidation was analyzed by Gas Chromatography (GC) as shown in Scheme 3.
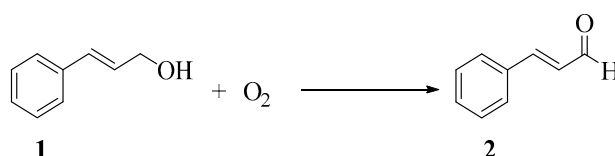
Scheme 3. Oxidation of cinnamyl alcohol (COH) to substituted cinnamaldehyde (CHO) with 0.1 g catalyst, 10 mL substrate solution at 70 °C in 60 min under vigorous stirring 1200 rpm using O_2 as oxidant.

After selective oxidation (selox) of cinnamyl alcohol (COH) to CHO the reactor is flushed with N_2 and 116.6 mg (1.07 mmol) OPD were loaded to same reactor in case of starting from COH, otherwise benzimidazole was synthesized from direct cyclization of CHO and OPD. The reaction mixture was stirred vigorously to obtain the desired product (E)-2-styryl-1H-benzo[d]imidazole (4a) and undesired product 1,2-di((E)-styryl)-1H-benzo[d]imidazole (4b) in case of using aqueous medium as shown in Scheme 4. The chemical reactions periodically monitored by TLC and all yields refer to isolated products. ^{1}HNMR in dimethyl sulfoxide DMSO-d$_6$ on a (DRX-600 ADVANCE) 600 MHz spectrometer

(Bruker, Zurich, Switzerland) were reported in ppm related to TMS. Mass spectra of product were analyzed on a Finnigan MAT 1020 (Thermo Fisher Scientific, Waltham, MA, USA) mass spectrometer operating at 70 eV. Infrared spectra of the products were recorded on a FT-IR Spectrometer (Tensor 37) by Bruker (Bruker, Zurich, Switzerland) in KBr with the absorption in cm^{-1}.
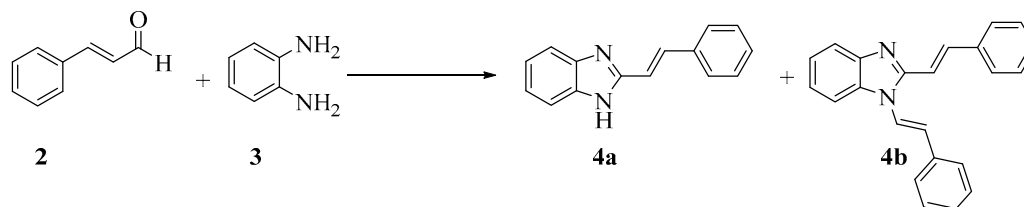
Scheme 4. CHO reaction with OPD (1.07 mmol) in solvents; ethanol, n-hexane, acetonitrile and water (10 mL) with catalyst (0.1 g) at 55 °C in 240 min under vigorous stirring.

3.6. Computational Studies

To investigate the theoretical-experimental consistency, quantum chemical calculations were performed using Gaussian 09 software. The complete geometry optimizations were done using the hybrid-density-functional B3LYP method [38] while employing 6-311++G(d, p) basis set. The minimized structures were assessed by frequency analysis to show whether or not the structures of these compounds represent true minimum energy geometries with no imaginary frequencies to ensure they don't represent transition states or other saddle points. Simple chemical reactivity descriptors were designed to calculate total energy (E), chemical hardness (η), electronic chemical potential (μ) and electrophilicity (ω) without laborious calculation. The resistance to change in the electron distribution or charge transfer is measured by the chemical hardness which associates with the stability and reactivity of a chemical system. On the basis of frontier molecular orbitals, chemical hardness corresponds to the gap between the highest occupied molecular orbital (HOMO; H) and lowest unoccupied molecular orbital (LUMO; L). Chemical hardness was approximated using Equation (1).

$$\eta = \frac{E_L - E_H}{2} \tag{1}$$

where E_L and E_H are the LUMO and HOMO energies. Electronic chemical potential was calculated using Equation (2).

$$u = \frac{E_L + E_H}{2} \tag{2}$$

Physically, μ defines the escaping tendency of electrons from an equilibrium system.

Electrophilicity index (ω), was calculated by using Equation (3) [39].

$$\omega = \frac{u}{2\eta} \tag{3}$$

4. Conclusions

In the current study, cinnamyl alcohol selectively oxidized to cinnamaldehyde over BNPs and BNPs/FMWCNTs at mild reaction conditions using solvents (ethanol, acetonitrile, and n-hexane), the reaction was extended for the synthesis of benzimidazole in the same pot efficiently. Substituted derivatives of benzimidazoles were synthesized from substituted OPD and CHO to explore the effect of substitution on the rate of reaction. An experimental and theoretical study revealed that the presence of methoxy substitution on OPD and nitro substitution on CHO increased percentage yield of benzimidazole from 73% to 98%. Among the catalysts used, Cu–Ti/FMWCNTs showed good performance for both cinnamyl alcohol oxidation and benzimidazole synthesis in ethanol at 55 °C in 240 min.

Author Contributions: Z.I. carried out the research, S.S. and A.A.K. performed the computational studies, M.S. was the PI of the project, I.U., Z.F., D.K. and N.B. helped in editing the initial draft, K.S. and F.M. helped in the sample characterization, M.A. helped in the editing and reviewing.

Conflicts of Interest: The authors declare no conflict of interest.

References

1. Arulmurugan, S.; Kavitha, H.P.; Venkatraman, B. Biological activities of Schiff base and its complexes: A review. *Rasayan J. Chem.* **2010**, *3*, 385–410.
2. Venkateswarlu, Y.; Kumar, S.R.; Leelavathi, P. Facile and efficient one-pot synthesis of benzimidazoles using lanthanum chloride. *Org. Med. Chem. Lett.* **2013**, *3*, 7. [CrossRef] [PubMed]
3. Hisano, T.; Ichikawa, M.; Tsumoto, K.; Tasaki, M. Synthesis of benzoxazoles, benzothiazoles and benzimidazoles and evaluation of their antifungal, insecticidal and herbicidal activities. *Chem. Pharm. Bull.* **1982**, *30*, 2996–3004. [CrossRef]
4. Kumar, B.V.S.; Vaidya, S.D.; Kumar, R.V.; Bhirud, S.B.; Mane, R.B. Synthesis and anti-bacterial activity of some novel 2-(6-fluorochroman-2-yl)-1-alkyl/acyl/aroyl-1H-benzimidazoles. *Eur. J. Med. Chem.* **2006**, *41*, 599–604. [CrossRef]
5. Vinodkumar, R.; Vaidya, S.D.; Kumar, B.V.S.; Bhise, U.N.; Bhirud, S.B.; Mashelkar, U.C. Synthesis, anti-bacterial, anti-asthmatic and anti-diabetic activities of novel N-substituted-2-(4-phenylethynyl-phenyl)-1H-benzimidazoles and N-substituted 2 [4-(4, 4-dimethyl-thiochroman-6-yl-ethynyl)-phenyl)-1H-benzimidazoles. *Eur. J. Med. Chem.* **2008**, *43*, 986–995. [CrossRef]
6. Mann, J.; Baron, A.; Opoku-Boahen, Y.; Johansson, E.; Parkinson, G.; Kelland, L.R.; Neidle, S. A new class of symmetric bisbenzimidazole-based DNA minor groove-binding agents showing antitumor activity. *J. Med. Chem.* **2001**, *44*, 138–144. [CrossRef]
7. Patil, A.; Ganguly, S.; Surana, S. A systematic review of benzimidazole derivatives as an antiulcer agent. *Rasayan J. Chem.* **2008**, *1*, 447–460.
8. Shah, K.; Chhabra, S.; Shrivastava, S.K.; Mishra, P. Benzimidazole: A promising pharmacophore. *Med. Chem. Res.* **2013**, *22*, 5077–5104. [CrossRef]
9. UŞ, C.K.; Altanlar, N. Synthesis of some new benzimidazole carbamate derivatives for evaluation of antifungal activity. *Turk. J. Chem.* **2003**, *27*, 35–40.
10. Mohamed, B.G.; Abdel-Alim, A.-A.M.; Hussein, M.A. Synthesis of 1-acyl-2-alkylthio-1, 2, 4-triazolobenzimidazoles with antifungal, anti-inflammatory and analgesic effects. *Acta Pharm.* **2006**, *56*, 31–48.
11. Kulkarni, M.V.; Patil, V.D. Synthesis Spectral Studies and Anti-Inflammatory Activity of Some New 2-Aryloxybenzimidazoles. *Arch. Pharm.* **1981**, *314*, 440–447. [CrossRef] [PubMed]
12. Mariappan, G.; Hazarika, R.; Alam, F.; Karki, R.; Patangia, U.; Nath, S. Synthesis and biological evaluation of 2-substituted benzimidazole derivatives. *Arab. J. Chem.* **2015**, *8*, 715–719. [CrossRef]

13. Stevenson, C.; Davies, R.J.H. Photosensitization of guanine-specific DNA damage by 2-phenylbenzimidazole and the sunscreen agent 2-phenylbenzimidazole-5-sulfonic acid. *Chem. Res. Toxicol.* **1999**, *12*, 38–45. [CrossRef] [PubMed]

14. Hasegawa, E.; Yoneoka, A.; Suzuki, K.; Kato, T.; Kitazume, T.; Yanagi, K. Reductive transformation of α, β-epoxy ketones and other compounds promoted through photoinduced electron transfer processes with 1, 3-dimethyl-2-phenylbenzimidazoline (DMPBI). *Tetrahedron* **1999**, *55*, 12957–12968. [CrossRef]

15. Figge, A.; Altenbach, H.J.; Brauer, D.J.; Tielmann, P. Synthesis and resolution of 2-(2-diphenylphosphinyl-naphthalen-1-yl)-1-isopropyl-1H-benzoimidazole; a new atropisomeric P, N-chelating ligand for asymmetric catalysis. *Tetrahedron Asymmetry* **2002**, *13*, 137–144. [CrossRef]

16. Savini, L.; Chiasserini, L.; Pellerano, C.; Filippelli, W.; Falcone, G. Synthesis and pharmacological activity of 1, 2, 4-triazolo [4, 3-a] quinolones. *II Farm.* **2001**, *56*, 939–945.

17. Chari, M.A.; Shobha, D.; Sasaki, T. Room temperature synthesis of benzimidazole derivatives using reusable cobalt hydroxide (II) and cobalt oxide (II) as efficient solid catalysts. *Tetrahedron Lett.* **2011**, *52*, 5575–5580. [CrossRef]

18. Rithe, S.; Jagtap, R.; Ubarhande, S. One pot synthesis of substituted benzimidazole derivatives and their characterization. *Rasayan J. Chem.* **2015**, *8*, 213–217.

19. Saberi, A. Efficient synthesis of Benzimidazoles using zeolite, alumina and silica gel under microwave irradiation. *Iran. J. Sci. Technol.* **2015**, *39*, 7–10.

20. Reddy, P.L.; Arundhathi, R.; Tripathi, M.; Rawat, D.S. CuI nanoparticles mediated expeditious synthesis of 2-substituted benzimidazoles using molecular oxygen as the oxidant. *RSC Adv.* **2016**, *6*, 53596–53601. [CrossRef]

21. Aman, R.; Sadiq, S.; Ali, M.; Sadiq, M.; Gul, J.; Saeed, K.; Khan, A.A.; Shah, S.H. Facile route for green synthesis of N-benzylideneaniline over bimetallic reduced graphene oxide: Chemical reactivity of 2, 3, 4-substituted derivatives of aniline. *Res. Chem. Intermed.* **2019**, *45*, 2947–2961. [CrossRef]

22. Trivedi, R.; De, S.K.; Gibbs, R.A. A convenient one-pot synthesis of 2-substituted benzimidazoles. *J. Mol. Catal. A Chem.* **2006**, *245*, 8–11. [CrossRef]

23. Srinivasulu, R.; Kumar, K.R.; Satyanarayana, P.V.V. Facile and efficient method for synthesis of benzimidazole derivatives catalyzed by zinc triflate. *Green Sustain. Chem.* **2014**, *4*, 33. [CrossRef]

24. Lu, J.; Yang, B.; Bai, Y. Microwave irradiation synthesis of 2-substituted benzimidazoles using PPA as a catalyst under solvent-free conditions. *Synth. Commun.* **2002**, *32*, 3703–3709. [CrossRef]

25. Riadi, Y.; Mamouni, R.; Azzalou, R.; El Haddad, M.; Routier, S.; Guillaumet, G.; Lazar, S. An efficient and reusable heterogeneous catalyst animal bone meal for facile synthesis of benzimidazoles, benzoxazoles, and benzothiazoles. *Tetrahedron Lett.* **2011**, *52*, 3492–3495. [CrossRef]

26. Kokare, N.D.; Sangshetti, J.N.; Shinde, D.B. One-pot efficient synthesis of 2-aryl-1-arylmethyl-1H-benzimidazoles and 2, 4, 5-triaryl-1H-imidazoles using oxalic acid catalyst. *Synthesis* **2007**, *2007*, 2829–2834. [CrossRef]

27. Chen, Y.X.; Qian, L.F.; Zhang, W.; Han, B. Efficient Aerobic Oxidative Synthesis of 2-Substituted Benzoxazoles, Benzothiazoles, and Benzimidazoles Catalyzed by 4-Methoxy-TEMPO. *Angew. Chem. Int. Ed.* **2008**, *47*, 9330–9333. [CrossRef]

28. Zada, N.; Khan, I.; Saeed, K. Synthesis of multiwalled carbon nanotubes supported manganese and cobalt zinc oxides nanoparticles for the photodegradation of malachite green. *Sep. Sci. Technol.* **2017**, *52*, 1477–1485. [CrossRef]

29. Shakirullah, M.; Ahamd, I.; Zada, N.; Ishaq, M.; Ahmad, W.; Saeed, K.; Mohammadzai, I.U. Thermocatalytic Conversion of Coal Soot to Carbon Nanorods, Fullerenes. *Fuller. Nanotub. Carbon Nanostruct.* **2013**, *21*, 171–182. [CrossRef]

30. Saeed, K.; Zada, N.; Khan, I. Photocatalytic degradation of alizarin red dye in aqueous medium using carbon nanotubes/Cu–Ti oxide composites. *Sep. Sci. Technol.* **2018**, 1–9. [CrossRef]

31. Monazzam, P.; Kisomi, B.F. Co/TiO$_2$ nanoparticles: Preparation, characterization and its application for photocatalytic degradation of methylene blue. *Desalin. Water Treat.* **2017**, *63*, 283–292.

32. Rekha, M.; Hamza, A.; Venugopal, B.; Nagaraju, N. Synthesis of 2-substituted benzimidazoles and 1, 5-disubstituted benzodiazepines on alumina and zirconia catalysts. *Chin. J. Catal.* **2012**, *33*, 439–446. [CrossRef]

33. Dhopte, K.B.; Zambare, R.S.; Patwardhan, A.V.; Nemade, P.R. Role of graphene oxide as heterogeneous acid catalyst and benign oxidant for synthesis of benzimidazoles and benzothiazoles. *RSC Adv.* **2016**, *6*, 8164–8172. [CrossRef]

34. Rajabi, F.; De, S.; Luque, R. An Efficient and Green Synthesis of Benzimidazole Derivatives Using SBA-15 Supported Cobalt Nanocatalysts. *Catal. Lett.* **2015**, *145*, 1566–1570. [CrossRef]

35. Baltork, I.M.; Moghadam, M.; Tangestaninejad, S.; Mirkhani, V.; Zolfigolb, M.A.; Hojatia, S.F. Silica Sulfuric Acid Catalyzed Synthesis of Benzoxazoles, Benzimidazoles and Oxazolo[4,5-b] pyridines Under Heterogeneous and Solvent-Free Conditions. *J. Iran. Chem. Soc.* **2008**, *5*, S6S–S70.

36. Senapak, W.; Saeeng, R.; Jaratjaroonphong, J.; Promarak, V.; Sirion, U. Metal free selective synthesis of 2-substituted benzimidazoles catalysed by Bronsted acidic ionic liquid: Convenient access to one pot synthesis of N-alkylated 1,2-disubstituted benzimidazoles. *Tetrahedron* **2019**, *75*, 3543–3552. [CrossRef]

37. Kalhor, M.; Mobinikhaledi, A.; Jamshidi, J. Synthesis of 2-arylbenzimidazoles catalyzed by transition metal nitrates. *Res. Chem. Intermed.* **2013**, *39*, 3127–3133. [CrossRef]

38. Becke, A.D. Density-functional thermochemistry. III. The role of exact exchange. *J. Chem. Phys.* **1993**, *98*, 5648–5652. [CrossRef]

39. Špirtović-Halilović, S.; Salihović, M.; Veljović, E.; Osmanović, A.; Trifunović, S.; Završnik, D. Chemical reactivity and stability predictions of some coumarins by means of DFT calculations. *Glas. Hem. Tehnol. Bosne Herceg.* **2014**, *43*, 57–60.